Kidney International, Vol. 47 (1995), pp. 1274–1284

Endocytosis and transcytosis of albumin gold through mice peritoneal mesothelium

LAZARO GOTLOIB and AVSHALOM SHOSTAK

Department of Nephrology and the Kornach Laboratory for Experimental Nephrology, Central Emek Hospital, Afula, Israel

Endocytosis and transcytosis of albumin-gold complexes through mice peritoneal mesothelium. The present transmission electron microscopy (TEM) study was designed to investigate whether mesothelial cells of mice diaphragmatic, parietal and mesenteric peritoneum are actively coupled to the mechanisms involved in the transerosal absorption of albumin gold complexes (Alb-Au). Five albino mice were injected intraperitoneally with 0.5 ml of a suspension of Alb-Au. In three animals, *in vivo* fixation was done 10 minutes after injection of Alb-Au, whereas in the remaining two, fixation was performed 45 minutes after injection of the tracer. At both time intervals, a substantial part of Alb-Au complexes was observed within plasmalemmal and coated vesicles, mainly attached to the luminal aspect of the internal luminal membranes. The amount of Alb-Au contained in plasmalemmal vesicles was significantly higher than that detected in intermesothelial junctions. Plasmalemmal vesicles were observed discharging Alb-Au complexes in the submesothelial interstitium, showing a significantly higher proportion of the tracer associated with non-junctional areas. Evidence presented in this study supports the idea of local degradation of Alb-Au in mesothelial cells after endocytosis, and that of a continuously transcytotic mechanism transporting polymerized albumin across the mesothelial layer. In this sense, transcytotic vesicles could represent the large pore equivalent.

The relevance of mesothelial cells in the transperitoneal transfer of substances in and out of the abdominal cavity is still debated [1]. Almost one century ago, it was demonstrated that absorption of serum from serous cavities takes place at a slower rate than that of isotonic sodium chloride solutions [2]. Then, it was postulated that absorption is dependent on the vital activity of the cells lining the serous cavities. This hypothesis found experimental support in more modern *in vitro* and *in vivo* studies. It has been demonstrated that absorption from the peritoneal cavity and transperitoneal passage of several small solutes are sensitive to temperature changes, drugs and metabolic inhibitors [3–6]. However, the mechanisms and pathways governing the peritoneal absorption of albumin from the peritoneal cavity have not been completely identified, in spite of the profuse published literature dealing with this specific subject. It has been proposed that peritoneal lymphatics are the main pathway for the drainage of absorbed albumin [7–10]. In this context, diaphragmatic lymphatics have been adscribed the role of channeling at least 60% of the total amount of peritoneal fluid and albumin, drained through the right lymph and thoracic ducts [8, 10]. This process of absorption has been described as occurring basically at the level of the diaphragmatic stomata [9], originally unfolded by Von Recklinghausen. However, the amount of lymph drained through visceral and parietal peritoneal lymphatics is still ill defined [11]. Furthermore, recent information [12, 13] suggests that peritoneal lymphatics may not play an exclusive role in the transport of absorbed albumin to the venous circulation.

The role of the mesothelial layer in the phenomenon of absorption has been considered both extremely important [1, 4, 6] and irrelevant [12]. Facing this controversy, we decided to investigate whether mesothelial cells of mouse diaphragmatic, parietal and mesenteric peritoneum are actively coupled to the mechanisms leading to the transerosal absorption of albumin. From the variety of techniques which have been applied to study localization of cellular macromolecules, we chose albumin gold complexes. This tracer is an electron-dense, non-cytotoxic and stable cytochemical marker [14]. Even though the nature of macromolecular binding to gold is largely unknown, it has been demonstrated that it is irreversible [15]. This technique has also been recently used to study *in vivo* endocytosis by endothelial cells of bone marrow sinusoid capillaries [16].

Therefore, bovine serum albumin gold complexes (Alb-Au) were used for detecting, by means of transmission electron microscopy (TEM), the transmesothelial transport of macromolecular proteins.

Methods

Five apparently healthy albino male mice, weighing 21 to 24 g, were intraperitoneally (i.p.) injected with 0.5 ml of albumin (bovine-biotin amido caproyl labeled) adsorbed to colloidal gold (Sigma) (Alb-Au complexes). Gold mean particle diameter estimated by TEM was 9.1 ± 0.7 nm (± SD) (coefficient of variation: 7.3%), according to data obtained by the manufacturer after measuring 100 gold particles. The average diameter of this polymeric albumin-gold complex is approximately of 14.4 nm [17]. The suspension was prepared in 50% glycerol containing 0.15 M NaCl, 0.01 M phosphate buffer, 5 mg/ml albumin, 0.05% Tween 20 at pH 7.0, and the number of particles was of 4.1×10^{13}/ml.

After a dwell time of 10 minutes, *in vivo* fixation of the peritoneum was carried out under ether anesthesia, injecting 5 ml of Karnovsky fixative [18] intraperitoneally. This solution was left to dwell for a period of 10 minutes, by the end of which samples of parietal, diaphragmatic and mesenteric peritoneum were surgically taken, after laparotomy, from each one of three animals. In

Received for publication July 6, 1994
and in revised form December 7, 1994
Accepted for publication December 8, 1994

the other two, the Alb-Au suspension was left to dwell for 45 minutes, and only thereafter was the procedure of *in vivo* peritoneal fixation carried out. Damage by handling the mesothelial surface was carefully avoided.

Tissue samples were sectioned to pieces of approximately 1 mm^3. Fixation was done by 2% formaldehyde and 2.5% glutaraldehyde in 0.1 M sodium cacodylate buffer at pH 7.2 and at a temperature of 4°C overnight. After rinsing in the same buffer, the samples were post-fixed in 2% osmium tetroxide for one hour, then dehydrated in ethanol and embedded in Epon 812. Three to four blocks from each examined peritoneal portion (mesentery, parietal and diaphragmatic peritoneum) were prepared. Consequently, 9 to 12 blocks were prepared from each mouse, making a total number of 51 blocks (28 from the 10-min dwell time, and 23 from the 45-min dwell animals).

Preliminary 1 μm semithin sections were cut from each block, stained with 1% toluidine blue, and examined by light microscopy. Areas containing mesothelium, blood and lymphatic capillaries were identified, and ultrathin sections were cut on a diamond knife using an LKB 4804 A ultramicrotome, mounted on copper grids, stained with lead citrate, and examined in a Phillips 300 electron microscope at 60 Kv.

The number of examined grids ranged between 4 and 5 per block, making a total number of 234 grids: 130 from the 10-minute dwell group, and 104 from the group where the dwell time of Alb-Au was 45 minutes.

For morphometric purposes, 25 electron micrographs (approximately 1 per block) were taken from the mesothelium covering the cavitary surface of each one of the explored peritoneal portions (mesentery, diaphragmatic and parietal peritoneum). Prints were enlarged to achieve a final magnification of ×41,500. Both length of the mesothelial cell's plasma membrane facing the abdominal cavity and surface area of cells cytoplasm appearing in the electron micrographs were measured by planimetry. Other measurements on the prints were made using a vernier caliper (accurate to 0.01 mm) and a hand magnifying lens.

Mean thickness of sectioned mesothelial and endothelial cells was calculated from measurements taken every 10 mm along the prints (so far, 10 mm/41,500 = 0.24 μm). Length and exposed area of sectioned mesothelium were not significantly different in both groups of data (10 and 45 min samples). The same can be stated for the individual contribution of each peritoneal portion to the total figures.

For the 10 minute samples, length of the examined mesothelial luminal border was 200.16 μm (mesentery, 71.45 μm; diaphragmatic mesothelium, 78.46 μm; parietal peritoneum, 50.25 μm), and the mean cellular thickness was 0.71 ± 0.38 μm (mesentery, 0.68 ± 0.62 μm; diaphragmatic mesothelium, 0.59 ± 0.31 μm; and parietal peritoneum, 0.86 ± 0.10 μm).

For samples obtained 45 minutes after the injection of Alb-Au, the total luminal length was 165.80 μm (mesentery, 50.26 μm; diaphragm, 63.37 μm; parietal peritoneum, 52.17 μm), whereas mean cell thickness was 0.67 ± 0.41 μm (mesentery, 0.55 ± 0.19 μm; diaphragm, 0.77 ± 0.61 μm; parietal peritoneum, 0.69 ± 0.43 μm).

The total area of transversal sections of mesothelial cells shown in the 10 minute sections was 138.17 μm^2 (mesentery, 48.61 μm^2; diaphragmatic mesothelium, 46.31 μm^2; parietal peritoneum, 43.25 μm^2). The total area assessed in mesothelial sections obtained 45 minutes after the intraperitoneal injection of Alb-Au complexes was 118.39 μm^2 (mesentery, 31.06 μm^2; diaphragmatic mesothelium, 50.25 μm^2; and parietal peritoneum, 37.07 μm^2). Thirty more photographs showing lymphatic capillaries were obtained on samples taken from diaphragmatic peritoneum: 15 at 10 minutes, and the other 15 at 45 minutes after i.p. injection of the Alb-Au complexes. Final prints were enlarged at ×41,500.

Table 1. Total numbers of Alb-Au particles observed in different parts of the peritoneal samples obtained from the 10 and the 45 minute dwell time groups

Samples	10 min	45 min	*P*
Total number of observed Alb-Au particles	1729	949	
Alb-Au on glycocalyx	248 (14.34%)	53 (5.58%)	< 0.001
Alb-Au into tight junctions (*percent of extracellular Alb-Au particles*)	(3.76%)	(0.53%)	< 0.01
Number of tight junctions with Alb-Au (*% of TJ*)	10/37 (27.03%)	3/34 (8.82%)	< 0.001
Intracellular Alb-Au	1252 (72.41%)	796 (83.88%)	< 0.001

Unless specified differently, numbers between parentheses indicate the percentage of the total number of observed Alb-Au particles.

The total luminal length of the examined lymphatic endothelium was 66.75 μm for the 10 minute samples, whereas for the 45 minute observations, figures were 50.27 μm. Mean endothelial cell thickness for the 10 and the 45 minute dwell time groups were 0.38 ± 0.24 μm and 0.32 ± 0.18 μm, respectively. The exposed area of sectioned lymphatic endothelium was 27.20 μm^2 in the 10 minute samples, and 17.55 μm^2 for the 45 minute specimens. Ten more electronmicrographs were taken from blood microvessels at each time interval.

Values are presented as mean ± standard deviation. Comparison between two percentages was performed according to the following formula:

$$Z = \frac{P1 - P2}{\sqrt{P(1 - P)[(1/n1) + (1/n2)]}}$$

$$\text{Whereas: } P1_{n1} = \alpha 1 \cdot P2_{n2} = \alpha 2$$

$\alpha 1$ and $\alpha 2$ are the observed percentages in groups 1 and 2, respectively, and n1 and n2 are number of cases in each group. $P = \alpha 1 + \alpha 2$ n1 + n2 [19].

The level of probability "*P*" was obtained by looking up the calculated value of parameter "Z" in the table of the normal distribution. The null hypothesis was rejected at a significance level of 0.05 (z parameter in the table of the normal distribution: 1.960).

Results

The mesothelial layer

Luminal aspect. Data presented in Table 1 indicate that the total number of Alb-Au complexes counted in the 10 minute samples was substantially higher than that observed at 45 minutes.

Intercellular junctions. Approximately 27% of the observed tight junctions showed Alb-Au in the 10 minute specimens, even though particles of the tracer were seen in the abluminal portion of the intercellular space in only six occasions (1.02% of extracellular Alb-Au). Table 1 shows that both groups of observations were made on an almost similar number of tight junctions.

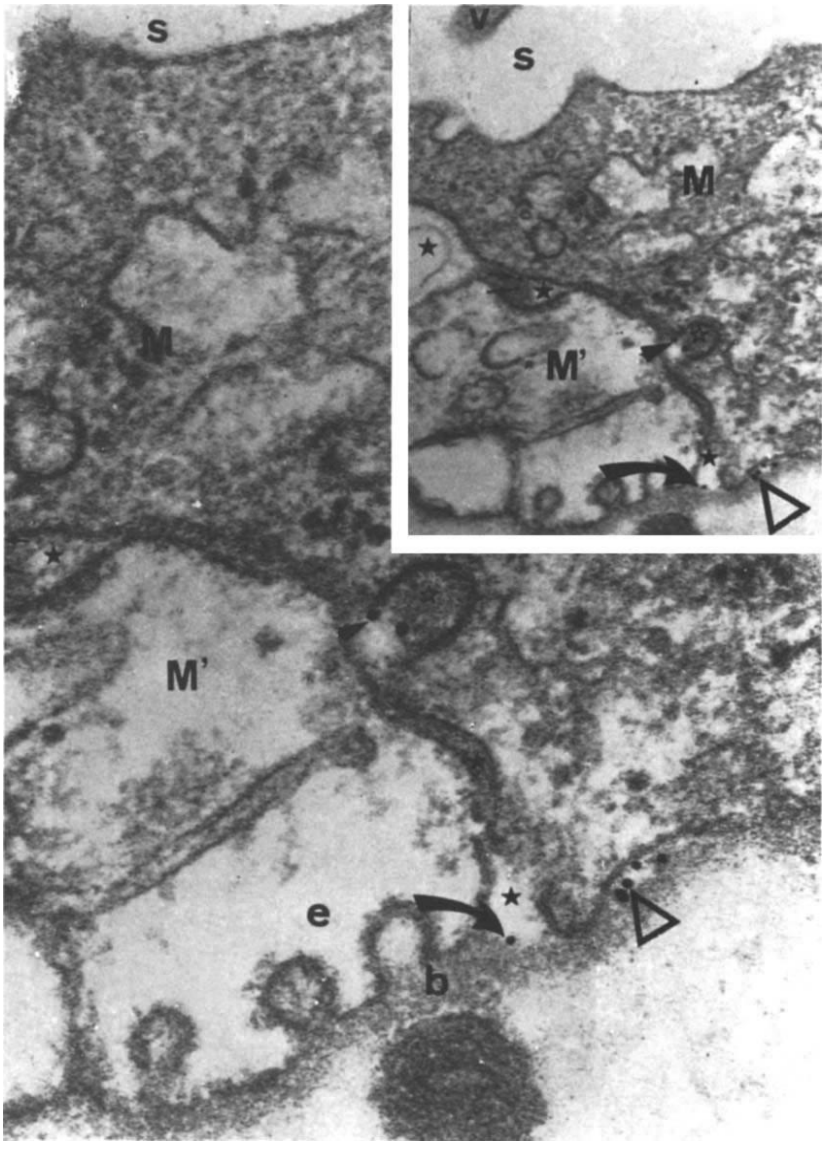

Fig. 1. *Parietal peritoneum (10 min after i.p. injection of Alb-Au).* Two adjoining mesothelial cells (M, M') demarcate an intercellular space (black stars) which contains Alb-Au complexes in both the luminal (short straight arrow) and the abluminal side of the channel. Plasmalemmal vesicle (open star) is open into the intercellular channel, through a neck containing Alb-Au complexes (black arrowhead). Particles of the tracer can be noticed on the abluminal side of the mesothelial cell (open arrowhead), within the space limited by the cell plasmalemma and the submesothelial basement membrane (b). One of the cells (M') shows areas of structureless edema (e). s is the peritoneal space. (× 87000). **Upper right inset.** The same photograph is presented at lower magnification to give a better look of the luminal mesothelial cell aspect (v is microvilli) (× 41500).

However, the absolute number and the proportion of junctions showing Alb-Au were significantly lower in specimens taken from the 45 minute group of animals. Indeed, in this last group, only two particles of the tracer (1.22% of extracellular Alb-Au) were observed in the abluminal portion of the junction. Occasionally (Fig. 1), adjoining cells showed evidence of substantial intracellular edema. This suggests some inefficiency in the homeostatic mechanisms that maintain cell volume and electrolyte concentration gradients across the cell membrane [20, 21] and, of course, a substantially reduced cellular vitality.

It should be noticed that the presence of Alb-Au complexes within an intermesothelial cell junction does not necessarily imply that the only possible pathway between cavity and interstitial space is through the intercellular channel. Indeed, Figure 1 shows an open plasmalemmal vesicle through the neck of which Alb-Au complexes are discharged into the intercellular channel.

At times, particles of the tracer were seen within open intercellular spaces separating two recently implanted mesothelial cells.

Mesothelial cells. The vast majority of Alb-Au particles was associated with the mesothelial cells. The absolute amount, as well as the percentage of total particles contacting the glycocalyx was significantly higher at 10 minutes (Table 1). Conversely, at 45 minutes, the percentage of particles disseminated within cells was higher than that observed at 10 minutes (Table 1).

Populations of pinocytotic vesicles at 10 and 45 minutes were not statistically different (818 at 10 min, and 752 in the 45 min samples). Furthermore, no significant differences in the topographical distribution of pinocytotic vesicles (luminal, abluminal, non-attached) were demonstrated.

The proportion of Alb-Au complexes included into pinocytotic vesicles (and calculated as percentage of intracellular tracer) was significantly higher ($P < 0.01$) in the 45 minute specimens (26.67% at 10 min, vs. 43.47% at 45 min). In addition, numbers

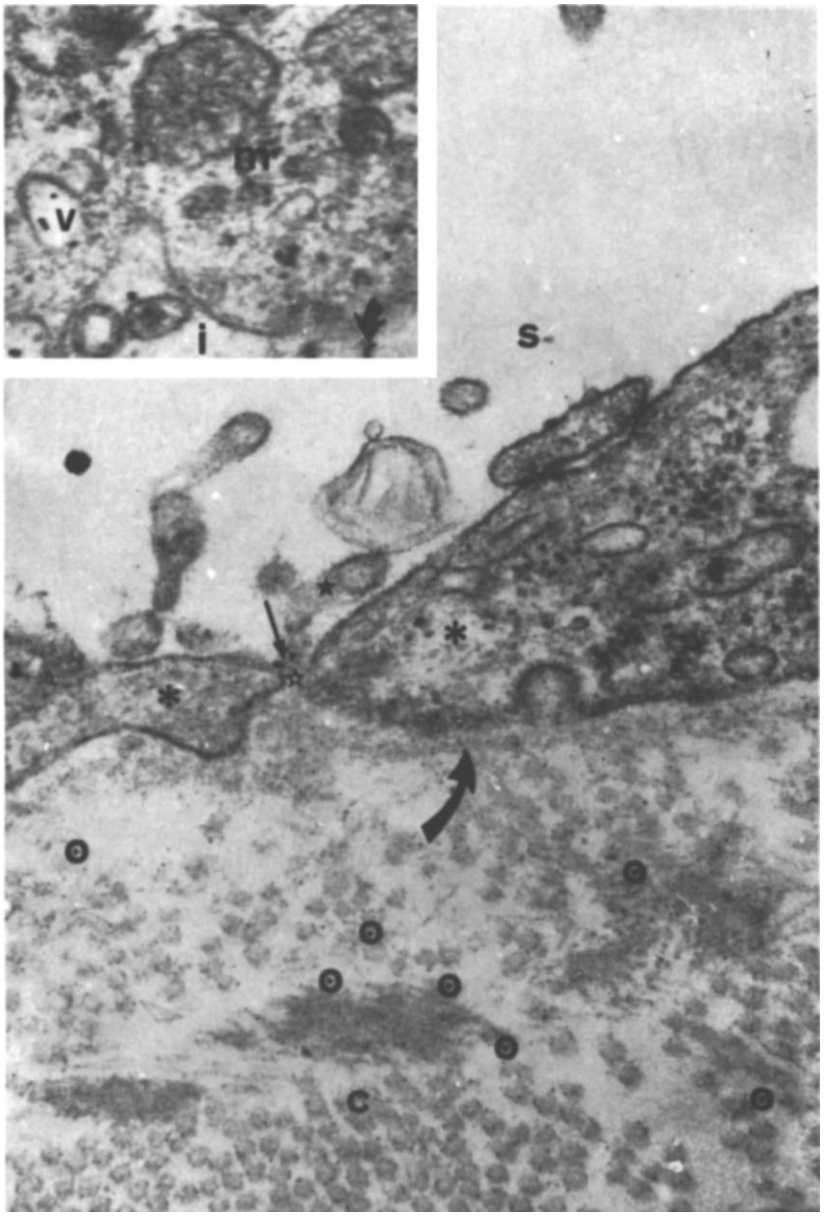

Fig. 2. *Mice diaphragmatic mesothelium 10 minutes after i.p. injection of Alb-Au complexes.* Note the presence of Alb-Au complexes (straight arrow) on the luminal aspect of an apparenty open intermesothelial cell junction (open arrow). The asterisks identify both mesothelial cells. Particles of the tracer (open circles) are between the collagen fibers (c) of the submesothelial interstitial space. Abbreviation and symbols are: s, abdominal space; black star, microvilli; curved arrow, submesothelial basement membrane (× 41500). **Upper left inset.** Abluminal side of mesothelial cell (m). Plasmalemmal vesicle (V) shows Alb-Au complexes lying on the luminal limiting membrane. Curved arrow points to particles of the tracer located in the submesothelial interstitial space (i) (× 50720).

and proportions of the pinocytotic vesicles containing particles of the tracer showed no significant differences when counts made on the 10 and 45 minute samples were compared.

Alb-Au particles were considered to be attached to the luminal aspect of the internal vesicular membrane when the distance between both structures was less than 0.01 μm. In this context, most of the tracer appeared attached to the luminal membrane of pinocytotic vesicles (88.32% in the 10 min samples, and 91.04% at 45 min) (Fig. 2, inset). Approximately 10% of the particles appeared randomly distributed into the lumen of plasmalemmal vesicles (Fig. 3), suggesting the possible existence of a fluid-phase uptake.

In the 10 minute samples, approximately 15% of vesicular Alb-Au appeared in non-attached vesicles. This pattern was remarkably higher in the 45 minute samples, where almost 36% of the endocytic tracer appeared in non-attached vesicles. This value was significantly higher ($P < 0.001$) than the 7.54% (4.27 + 3.27%) of Alb-Au particles present in luminal and abluminal vesicles.

A high proportion of multivesicular bodies and endosomes (Fig. 4, inset) (71.43% at 10 min and 57.28% at 45 min) contained Alb-Au complexes. These organelles were observed near both the luminal and the abluminal aspect of mesothelial cells. Densities at 10 and 45 minutes were not significantly different.

Most coated pits from the 10 minute samples (82%) showed Alb-Au complexes attached to the luminal plasmalemma, whereas at 45 minutes no such cellular organelle carrying particles of the tracer was observed. This reduction was coincidental with the significant decrease of Alb-Au observed in glycocalyx at the same time interval. So far, it may be derived that at 45 minutes the endocytosis of Alb-Au may have been almost complete.

Although the number of coated vesicles found in both groups of

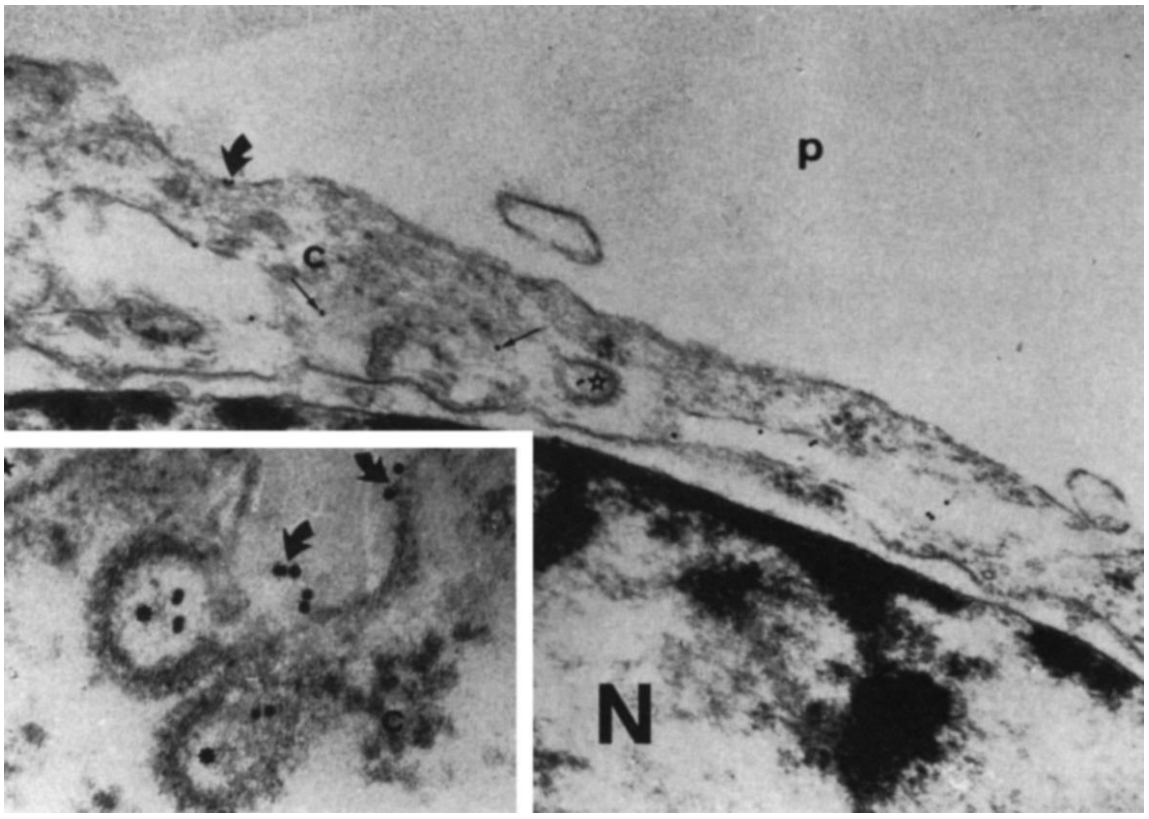

Fig. 3. *Parietal peritoneum 10 minutes after i.p. injection of Alb-Au.* Mesothelial cell (c) showing particles of the tracer within a coated vesicle (open star) in the cytoplasm (small straight arrows), as well as on the luminal plasmalemma (short curved arrow). Abbreviations are: p, peritoneal space; N, nucleus of mesothelial cell (× 41500). **Low left inset.** Other area of the same mesothelial cell at higher magnification. Coated vesicles (asterisks) show Alb-Au complexes (arrows), most of them adsorbed on the luminal aspect of the limiting membrane. Black star, peritoneal space; C, cytoplasm of mesothelial cell (× 87000).

samples were similar, the proportion of Alb-Au complexes included at 45 minutes (8.7%) was significantly higher ($P < 0.01$) than that observed at 10 minutes (2.3%). As for plasmalemmal vesicles, most particles of the tracer were attached to the luminal aspect of the internal limiting membrane of coated vesicles (90% at 10 min, and 61.43% at 45 min; P = NS). Few Alb-Au was observed free in mesothelial cell cytoplasm. The proportions were 1.52% and 0.5% of total intracellular Alb-Au for the 10 and the 45 minute samples (P = NS).

Alb-Au complexes in the submesothelial interstitial tissue. As early as 10 minutes after being injected, Alb-Au was noticed in the submesothelial interstitial space lying between the cell and its basement membrane (Figs. 1 and 2, inset), and even distant, between collagen fibers located under the mesothelium (Fig. 2), as well as among those adjacent to lymphatic capillaries (Fig. 4). The mean distance separating interstitial Alb-Au complexes from abluminal aspect of mesothelial cell plasmalemma was 0.27 ± 0.26 μm (range 0.01 to 1.86 μm) at 10 minutes and 0.28 ± 0.31 μm (range 0.001 − 1.03 μm) for the 45 minute samples.

Ten minutes after intraperitoneal injection, almost 6% of the total number of observed Alb-Au complexes found its way to the submesothelial interstitial tissue. Very few of them appeared close to junctional areas. At 45 minutes, the proportion of Alb-Au complexes located within the interstitial compartment was higher than that observed at 10 minutes, even though the difference did

Table 2. Alb-Au complexes in submesothelial interstitial tissue and in mesothelial intercellular junctions and plasmalemmal vesicles

	10 min	45 min	*P*
Interstitial Alb-Au complexes	107 (5.82%)	90 (9.38%)	NS
Alb-Au complexes in junctional areas (excluding diaphragmatic stomata)	4 (0.21%) (1 = parietal 3 = diaphragm)	8 (0.83%) (2 = parietal 1 = mesentery 5 = diaphragm)	NS
Alb-Au in diaphragmatic stomata	7 (0.38%)	11 (1.15%)	NS
Alb-Au in non-junctional areas	100 (5.44%)	79 (8.23%)	NS
Non-junctional vs. junctional Alb-Au (10 min)	5.44% vs. 0.59%	—	< 0.05
Non-junctional vs. junctional Alb-Au (45 min)	—	8.23% vs. 1.15%	< 0.05
Alb-Au in plasmalemmal vesicles vs. those observed in tight junctions at 10 min	18.16% vs. 3.53%	—	< 0.002
Alb-Au in plasmalemmal vesicles vs. those observed in tight junctions at 45 min	—	36.04% vs. 0.52%	< 0.001

Values between parentheses represent percentages of total number of observed Alb-Au complexes.

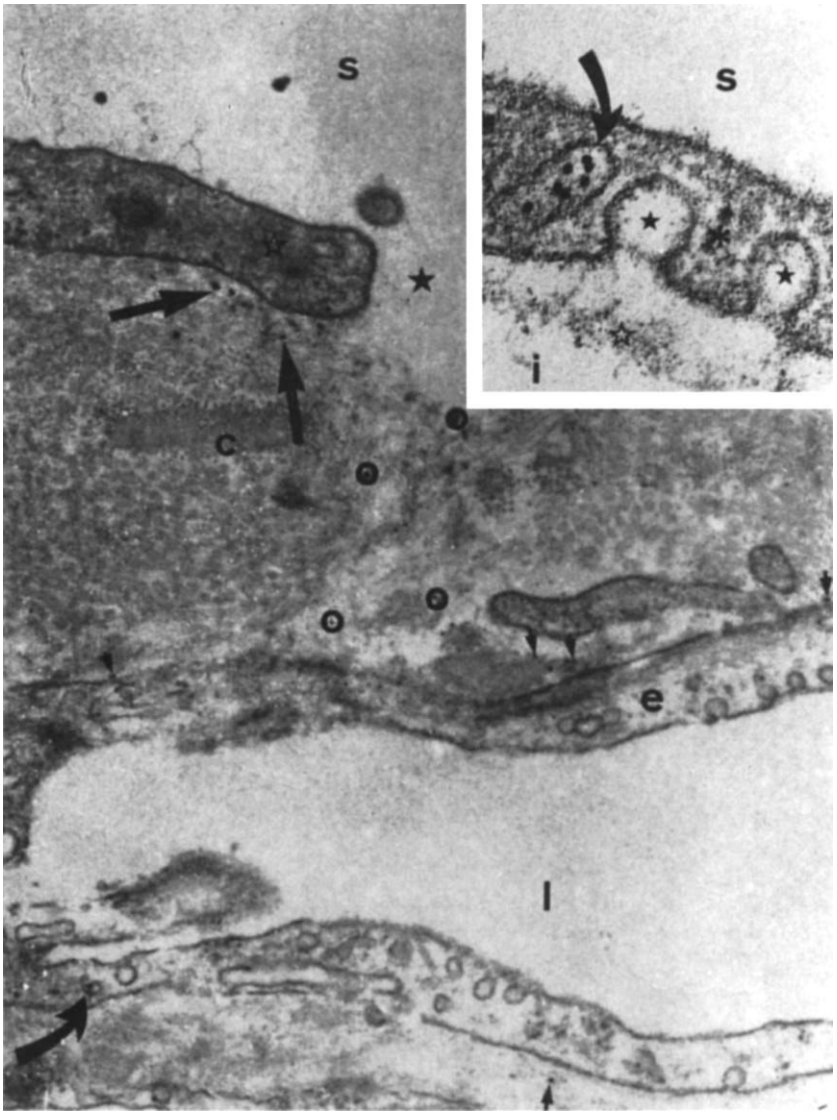

Fig. 4. *Diaphragmatic peritoneum 10 minutes after i.p. injection of Alb-Au complexes.* The black star calls attention to a stomata communicating the peritoneal space (s) and the submesothelial connective tissue (c). Alb-Au complexes (large straight arrow) are present immediately under the mesothelial cell (open arrow), between collagen fibers (open circles), as well as in the subendothelial interstitial space (short straight arrows) of the lymphatic lacuna. The curved arrow points at a particle of the tracer included in an endothelial plasmalemmal vesicle (e is lymphatic endothelial cell). (× 30740). **Inset.** Diaphragmatic mesothelium 10 min after i.p. injection of Alb-Au complexes. Arrow indicates an endosome containing Alb-Au complexes. Abbreviations and symbols are: s, peritoneal space; *, mesothelial cell cytoplasm; black stars, plasmalemmal vesicles; open star, submesothelial basement membrane; i, interstitial space (× 64550).

not reach statistical significance (Table 2). Here again, less than 10% of the observed Alb-Au was adjacent to junctional areas. It should be noted that at both time intervals, percentages of non-junctional interstitial Alb-Au complexes were significantly higher than those appearing close to the abluminal side of intercellular junctions (Table 2).

Morphologically, intermesothelial cell gaps of diaphragmatic stomata appeared as open pathways for Alb-Au complexes (Fig. 4), even though their capability of delivering particles of the tracer to the lymphatic system did not seem much higher than that shown by non-stomatal mesothelial junctions (Table 2). On the whole, it can be inferred from the last two statistical comparisons presented in Table 2 that the proportion of Alb-Au complexes observed into plasmalemmal vesicles is significantly higher than that found within intermesothelial cell junctions.

Diaphragmatic lymphatic capillaries

Microvascular lumen, glycocalyx and interendothelial cell junctions. Comparison of the total number of Alb-Au complexes within the microvascular lumen as well as that of particles observed per micron of luminal glycocalyx in samples obtained at 10 and 45 minutes did not show significant differences. Modest and almost much the same proportions of Alb-Au complexes were observed passing through open interendothelial cell junctions at both intervals (Fig. 5; 3.88% at 10 min vs. 2.59% at 45 min; P = NS).

The interstitial density of the tracer appeared significantly higher in the 10 minute samples, whereas most of it was distributed along non-junctional areas of the endothelial abluminal aspect (Table 2).

The presence of Alb-Au complexes in plasmalemmal vesicles and multivesicular bodies of lymphatic endothelial cells. Endothelial cells of lymphatic capillaries showed plasmalemmal vesicles, the total number and topographic distribution of which, at both time intervals, were not significantly different (data not shown).

Approximately one fifth of those vesicles contained Alb-Au complexes that were infrequently seen attached to the vesicle luminal limiting membrane (Fig. 4). Mostly the tracer appeared

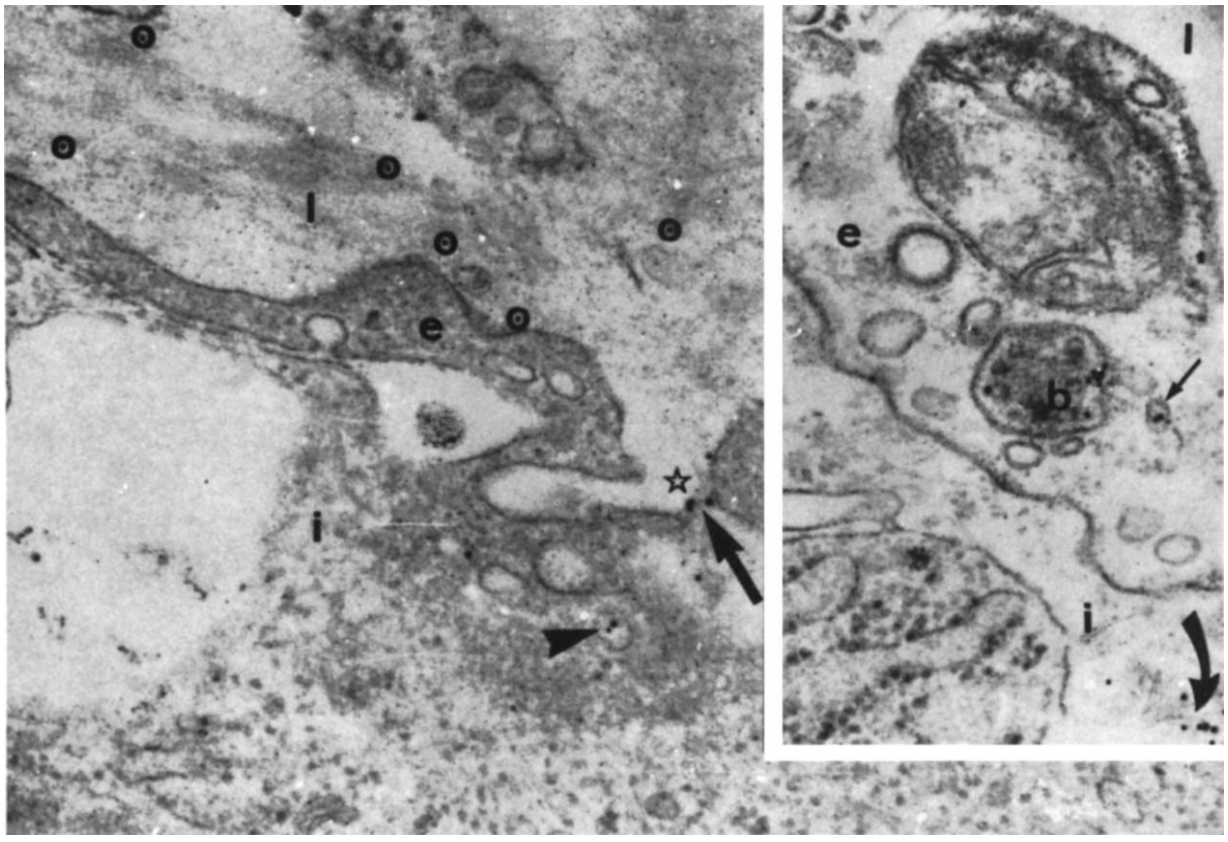

Fig. 5. *Diaphragmatic submesothelial lymphatic capillary 10 min after i.p. injection of Alb-Au complexes).* **Left inset.** Alb-Au complexes (long arrow) can be observed in their pathway through an open interendothelial cell junction (open star). More particles of the tracer are seen (open circles) within the luminal space (l) of the microvessel. Arrowhead points to Alb-Au included into a plasmalemmal vesicle (i is the subendothelial interstitium) (× 41500). **Right inset.** Lymphatic capillary endothelial cell (e). Alb-Au complexes appear into an endosome (b) as well as into a plasmalemmal vesicle (straight arrow). Curved arrow points at Alb-Au complexes present in the interstitium (i). Notice the absence of subendothelial basement membrane (× 64550).

Table 3. Distribution of Alb-Au complexes within the lumen, along the glycocalyx, in interendothelial cell junctions and interstitium of diaphragmatic lymphatic capillaries, at 10 and 45 minutes after i.p. injection of the tracer

	10 min	45 min	*P*
Alb-Au in subendothelial interstitium	41 (17.67%)	7 (3.65%)	< 0.01
Percentage of interstitial Alb-Au located in non-junctional areas	87.20%	100%	NS
Alb-Au in junctions vs. Alb-Au in PV (percentages of total Alb-Au counted complexes)	3.88% vs. 24.35%	—	< 0.001
	—	2.59% vs. 18.48%	< 0.001

Numbers between parentheses represent percentages of the total number of Alb-Au complexes observed in diaphragmatic lymphatics, unless otherwise specified.

Table 4. Plasmalemmal vesicles in endothelial cells of diaphragmatic lymphatic capillaries

	10 min	45 min	*P*
Alb-Au complexes within PV	56 (24.35%)	39 (18.48%)	NS
PV containing Alb-Au complexes	39 (16.96%)	15 (7.11%)	< 0.01
Alb-Au adsorbed on luminal aspect of PV internal limiting membrane	17.83%	15.28%	NS
Alb-Au complexes in MVB	77 (33.19%)	98 (51.04%)	< 0.001

Values between parentheses represent percentages of total counts of Alb-Au complexes.

free within the lumen of plasmalemmal vesicles (Fig. 5). There were no significant differences in density of labeling and topography of plasmalemmal vesicles, comparing data obtained at 10 and 45 minutes (data not shown). The proportion of Alb-Au complexes detected within plasmalemmal vesicles was significantly higher than those observed into interendothelial cell junctions at both time intervals (Table 3). Percentages of Alb-Au containing plasmalemmal vesicles were substantially higher in the 10 minute samples (Table 4).

Hence, multivesicular bodies (Figs. 4 and 6, inset) or endosomes containing Alb-Au complexes (Fig. 5, inset) were more frequently observed in samples obtained at 45 minutes (Table 4). At times, those organelles were noticed occupying most of the endothelial cell width. On a small scale, transcellular channels carrying Alb-Au complexes at times were observed connecting, apparently, the subendothelial interstitium with the microvascular lumen. Very occasionally (less than 0.1% of total counts), some

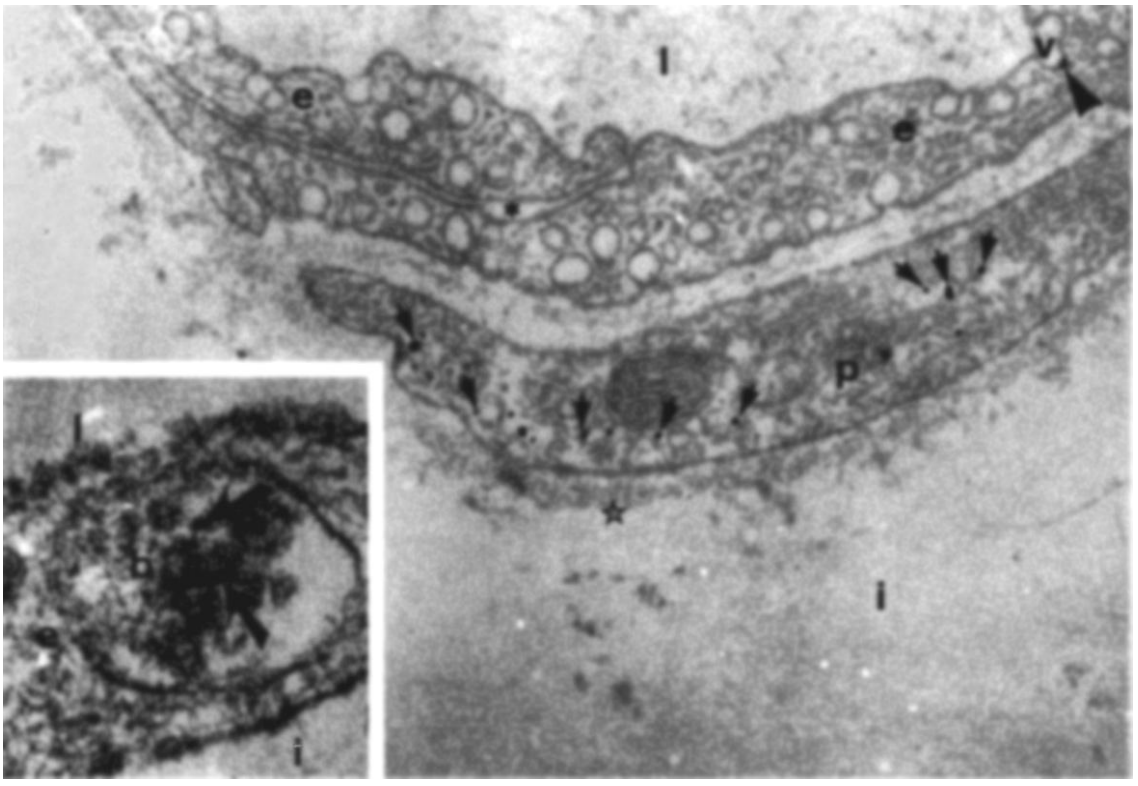

Fig. 6. *This post-capillary venule was observed in a sample of mesentery taken from a mouse 45 minutes after intraperitoneal injection of Alb-Au.* The intercellular junction (*) occurs between two adjacent endothelial cells (e). Alb-Au can be seen (arrowhead) adsorbed on the limiting membrane of a plasmalemmal vesicle (v) open on the microvascular lumen (l). The perithelial cell (p) shows plasmalemmal vesicles containing Alb-Au particles (arrows). Alb-Au is also visible (open star) in the subperithelial interstitial space (i) (× 33557). **Inset.** This micrograph of a lymphatic mesenteric capillary was taken on a sample obtained 45 minutes after intraperitoneal injection of Alb-Au. A multivesicular body (b) containing particles of Alb-Au (arrows) occupies a large part of the endothelial cell (e) thickness. Abbreviations are: l, microvascular lumen; i, interstitial space (× 87000).

Alb-Au complexes were observed free in the endothelial cell cytoplasm.

It should be emphasized that endothelial cells of blood capillaries observed in peritoneal samples obtained 10 minutes after injection of Alb-Au were in no instance decorated by particles of the tracer. Conversely, at 45 minutes Alb-Au complexes were present in plasmalemmal vesicles of blood capillary endothelium as well as in those located in perithelial cells of post-capillary venules. By the same time, Alb-Au complexes appeared in the interstitial tissue adjacent to blood microvessels (Fig. 6).

Discussion

The actual pathways and mechanisms by which macromolecular transport across microvascular endothelium and mesothelium occurs still remain to be identified. Some 50 years ago, it was suggested that junctions between capillary endothelial cells should be considered the main pathway for exchanges across the microvascular wall [22]. This concept was later on extended to the peritoneum, and was extensively analyzed within the frame of the one pore [23], the two pore [24, 25], and lately the three pore [26] size models of capillary and/or peritoneal permeability. The fact that these models failed to completely explain experimental data regarding the microvascular permeability to macromolecules lead some investigators to look for other possible mechanisms of transendothelial transport [27]. Furthermore, to date the endothelial and mesothelial postulated pores have not been convincingly identified. So, the existence of transcellular pathways via shuttling [27], or fused plasmalemmal vesicles [28] forming short-lived transendothelial channels [29–31] have been more recently proposed to explain the passage of macromolecular plasma proteins. Of course, both aforementioned mechanisms are not necessarily exclusive.

Albumin gold complexes are large compounds which apparently behave like polymerized albumin, and can be used as an electron microscope probe for the long time predicted and still unidentified large pore equivalent.

These complexes have been recently used for investigating receptor mediated endocytosis of albumin in several microvascular endothelia [32–37]. This approach, applied to the mouse mesentery, was expected to disclose whether injected Alb-Au would eventually be absorbed from the peritoneal cavity, by a process of endocytosis and, perhaps, transcytosis occurring through mesothelial cells. In this context, our observations show different moments of the process of transmesothelial absorption of the tracer. Ten minutes after the intraperitoneal injection of Alb-Au, the marker was present in coated pits and coated vesicles, in plasmalemmal vesicles, as well as in multivesicular bodies and endosomes of mesothelial cells.

Percentage of plasmalemmal vesicles carrying Alb-Au complexes ranged between 17.4% at 10 minutes and 16.22% at 45 minutes. Those figures are quite close to the 16% observed by

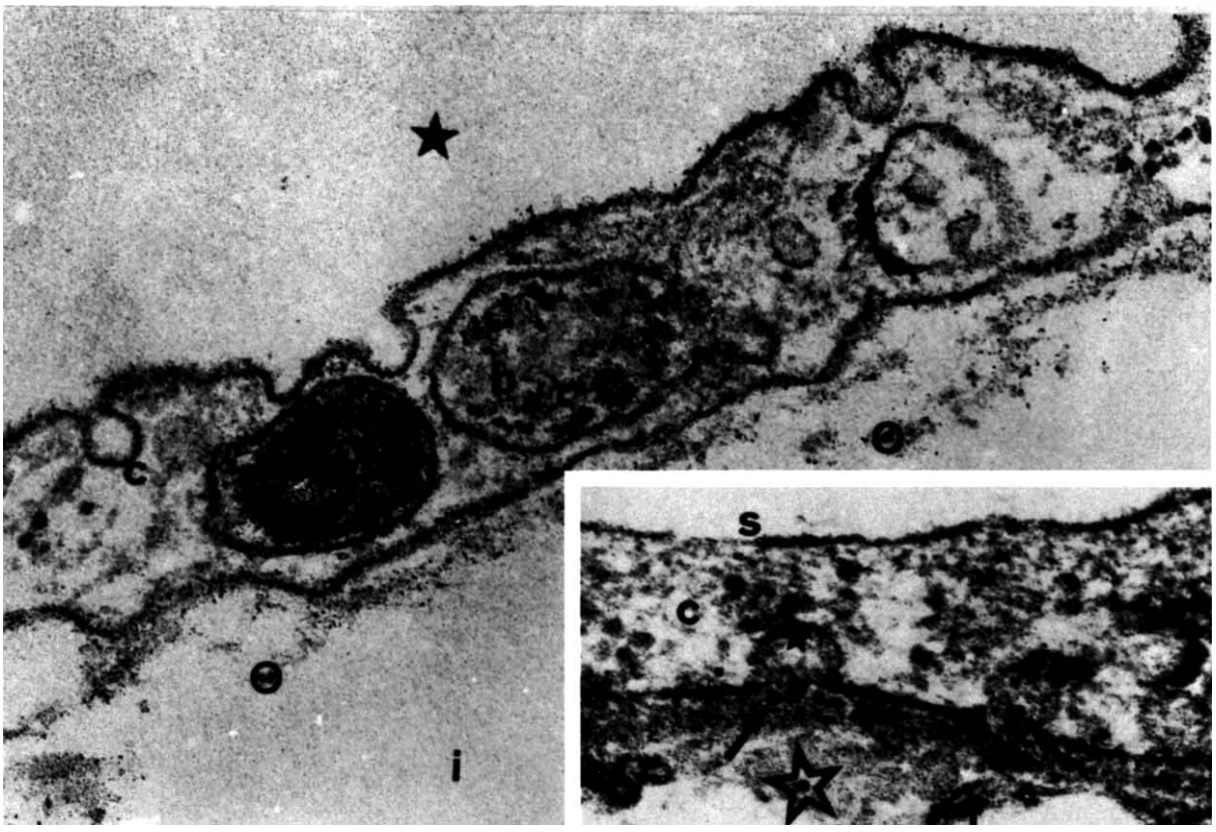

Fig. 7. *Sample of rat diaphragmatic mesothelium taken 10 minutes after intraperitoneal injection of Alb-Au.* The mesothelial cell (c) shows an endosome (b) containing numerous particles of the tracer. Other particles can be seen (open circles) in the submesothelial interstitium (i). Black star is the peritoneal space (× 64550). **Inset.** Other aspect of the same sample. Two abluminal plasmalemmal vesicles (black stars) were detected discharging Alb-Au particles (black arrows) in the submesothelial interstitium (i), which shows one particle of the tracer (open star) well beyond the basement membrane (*). Abbreviations are: S, peritoneal space; C, mesothelial cell (× 84530).

Milici et al [17] during receptor mediated transcytosis of monomeric albumin in mice myocardial capillary endothelium. This similarity leads to a speculation about the possibility that in our experiment, peritoneal absorption of the ligand took place mainly transcellularly by both endocytosis and transcytosis. The former mechanism would imply an active role of mesothelial cells in the degradation of at least conformationally modified albumins, as described by Schnitzer and Bravo [38]. The latter is also suggested by images showing abluminal plasmalemmal vesicles discharging Alb-Au complexes in the interstitial tissue separating the mesothelial cell from the subjacent basement membrane (Fig. 7).

It may be speculated that interstitial gold particles may eventually result from exocytosis of gold particles that have lost their albumin coating by lysosomal degradation. However, the chances are against this hypothesis since Milici et al [17] demonstrated that BSA remained attached to gold particles throughout the whole process of transcytosis through mice myocardial capillary endothelium.

As shown in Table 2, the proportion of tracer present in mesothelial junctions at 45 minutes was significantly higher than that observed in the 10 minute specimens. This may be a suggestion that a small percentage of Alb-Au reached the interstitium through junctions, but at a quite slow pace. This is in accordance with previous studies that demonstrated the existence of dense labeling of anionic sites [39–41] in clefts of intermesothelial cells, as well as within the portals and cellular surfaces bordering the stomatal openings [39], thus opposing the passage of anionic albumin. In this sense, the apparently direct communication between the abdominal cavity with the diaphragmatic lacunae and lymphatic capillaries [42] does not imply the existence of an absolutely open and free pathway. The relevance of the paracellular pathway is further diminished by the observation that percentage of Alb-Au appearing in junctional interstitial areas was remarkably lower than that detected in submesothelial tissue far off from abluminal side of intercellular junctions (Table 2).

All this information suggests that absorption of the ligand took place mainly transcellularly by both endocytosis and transcytosis. The proportional contribution of each mechanism cannot be evaluated. We do not yet know whether the interaction between Alb-Au complexes and mesothelial plasmalemmal and vesicular membranes is of a pure electrostatic nature or if it results from the presence of specific albumin binding proteins similar to those described in endothelial cells of mice capillaries obtained from several microvascular beds [33, 34, 37, 38, 43].

Samples taken at 45 minutes showed Alb-Au complexes in endothelial and perithelial cell vesicles of blood microvessels, as well as in the pericapillary interstitial tissue (Fig. 6). Of course, the information provided by the present experiments is insufficient to conclude about the direction of the passage. However, it should

be noted that 45 minutes elapsed since the intraperitoneal injection of the tracer which, on the other hand, was not observed in blood capillary endothelium at 10 minutes. Therefore, it is tempting to speculate that those Alb-Au complexes may well be particles of the tracer which, after being absorbed by peritoneal lymphatics, reached the mesentery again through the systemic circulation.

It has been estimated that the amount of albumin absorbed from the abdominal cavity through mesenteric lymphatics represents a quite small proportion of the whole peritoneal absorption [11]. However, our observations, together with the fact that mesenteric peritoneum makes up approximately 15% of the peritoneal surface [44], suggest that albumin absorption through mesenteric mesothelium appears to be substantially higher than previously thought. A similar deduction can be extended to parietal peritoneum, on the basis of the observations made on mesothelial cells covering the cavitary aspect of the abdominal cavity.

The present study suggests that mesothelial and capillary lymphatic endothelial cells are actively involved in the process of a pathway, which appears to be transcytosis by means of plasmalemmal vesicles and, at a minor degree, coated vesicles. If so, these organelles may well represent the equivalent of the postulated large pore. The fact that a few Alb-Au carrying transcellular channels were detected in lymphatic endothelium is a suggestion that this path, which is supposed to provide the convective component of the transcellular transport of large (>10 nm) solutes [17], is a minor element of the transendothelial transport system of the tracer.

Our findings also support the theory of vesicular transport for absorption of albumin, at least for the mesothelium and lymphatic endothelium [45]. The eventual role of intra-abdominal hydrostatic pressure within the range of values observed in clinical peritoneal dialysis [46], upon this specific process of albumin absorption [7, 10–13] by endocytosis and transcytosis, is still unclear [47]. The relevance of intermesothelial cell junctions seems to be minor, although this path can eventually become highly permeable to anionic plasma proteins during the acute inflammatory reaction. Under these circumstances, tight junctions appear to be wide open [48, 49], whereas the density of submesothelial anionic sites is substantially reduced [50].

This situation of having the mesothelium playing an active and vital role in the absorption from the peritoneal cavity [2] raises the possibility of modulating this process by means of pharmacological agents acting at the molecular level.

Finally, the active involvement of mesothelium, similar to that observed in vascular endothelial monolayers [51], supplemented to the lack of subendothelial lymphatic anionic sites, could be an additional explanation of the postulated asymetry in the bidirectional transport of macromolecules from blood to the peritoneal cavity, and from the cavity through the lymphatic system back to blood [12, 52].

Reprint requests to Lazaro Gotloib, M.D., Department of Nephrology, Central Emek Hospital, Afula 18101, Israel.

References

1. GOTLOIB L, OREOPOULOS DG: Transfer across the peritoneum: Passive or active? *Nephron* 29:201–202, 1981
2. STARLING EH, TUBBY AH: On absorption from and secretion into the serous cavities. *J Physiol* (London) 16:140–155, 1894
3. CLARK AJ: Absorption from the peritoneal cavity. *J Pharmacol Exp Ther* 16:415–433, 1921
4. BERNDT WO, GOSSELIN RE: Physiological factors influencing radiorubidium flux across isolated rabbit mesentery. *Am J Physiol* 200:454–458, 1961
5. CASCARANO J, RUBIN AD, CHICK WI, ZWEIFACH BW: Metabolically induced permeability across mesothelium and endothelium. *Am J Physiol* 206:373–382, 1964
6. RASIO EA: Metabolic control of permeability in isolated mesentery. *Am J Physiol* 226:962–968, 1974
7. ALLEN L, VOGT E: A mechanism of lymphatic absorption from serous cavities. *Am J Physiol* 119:776–782, 1937
8. COURTICE FC, ROBERTS DCK: Peritoneal fluid in the rabbit: Permeability of mesothelium to proteins, lipoproteins and acid hydrolases. *Lymphology* 8:1–10, 1975
9. TSILIBARRY EC, WISSIG SL: Lymphatic absorption from the peritoneal cavity: Regulation of patency of mesothelial stomata. *Microvasc Res* 25:22–39, 1983
10. MACTIER RA, KHANNA R, TWARDOWSKI ZG, NOLPH KD: Role of peritoneal cavity lymphatic absorption in peritoneal dialysis. *Kidney Int* 32:165–172, 1987
11. COURTICE FC, STEINBECK AW: The lymphatic drainage of plasma from the peritoneal cavity of the cat. *Aust J Exp Biol Med Sci* 28:161–169, 1950
12. FLESSNER MF: Peritoneal transport physiology: Insights from basic research. *J Am Soc Nephrol* 2:122–135, 1991
13. NAGY JA: Lymphatic and non lymphatic pathways of peritoneal absorption in mice: Physiology versus pathology. *Blood Purif* 10:148–162, 1992
14. GOODMAN SL, HODGES GM, TREJDOSIEWICZ LK, LIVINGSTON DC: Colloidal gold markers and probes for routine application in microscopy. *J Microsc* 123:201–213, 1981
15. HORISBERGER M, ROSSET J: Colloidal gold, a useful marker for transmission and scanning electron microscopy. *J Histochem Cytochem* 25:295–305, 1977
16. GEOFFREY JS, BECKER RP: Endocytosis by endothelial phagocytes: Uptake of bovine serum albumin-gold in bone marrow. *J Ultrastruct Res* 89:223–239, 1984
17. MILICI AJ, WATROUS NE, STUKENBROK H, PALADE GE: Transcytosis of albumin in capillary endothelium. *J Cell Biol* 105:2603–2612, 1987
18. KARNOVSKY MJ: A formaldehyde-glutaraldehyde fixative of high osmolality for use in electron microscopy. (abstract) *J Cell Biol* 27:137A, 1965
19. GLANTZ SA: *Primer of Bio-Statistics.* New York, McGraw-Hill, 1992, p 121
20. MACNIGHT ADC, LEAF A: Regulation of cellular volume. *Physiol Rev* 57:510–573, 1977
21. BERNDT WO, GOSSELIN RE: Differential changes in permeability of mesentery to rubidium and phosphate. *Am J Physiol* 202:761–767, 1962
22. CHAMBERS R, ZWEIFACH BW: Capillary cement in relation to permeability. *J Cell Comp Physiol* 15:255–272, 1940
23. PAPPENHEIMER JR: Passage of molecules through capillary walls. *Physiol Rev* 33:387–423, 1953
24. GROTTE G: Passage of dextran molecules across the blood-lymph barrier. *Acta Chirurg Scand* 211 (Suppl):1–84, 1956
25. NOLPH KD: The peritoneal dialysis system. *Contrib Nephrol* 17:44–49, 1979
26. RIPPE B: A three-pore model of peritoneal transport. *PD Int* 13 (Suppl 2):S33–S38, 1993
27. PALADE GE: Transport in quanta across the endothelium of blood capillaries. (abstract) *Anat Rec* 116:254, 1960
28. CLOUGH G, MICHEL CC: The role of vesicles in the transport of ferritin through frog endothelium. *J Physiol* (London) 315:127–142, 1981
29. BENDAYAN M, SANDBORN E, RASIO E: Studies of the capillary basal lamina. I. Ultrastructure of the red body of the eel swimbladder. *Lab Invest* 37:757–767, 1975
30. GHITESCU L, BENDAYAN M: Transendothelial transport of serum albumin: A quantitative immunocytochemical study. *J Cell Biol* 17: 745–755, 1992

31. CASLEY-SMITH JR, CHIN JC: The passage of cytoplasmic vesicles across endothelial and mesothelial cells. *J Microsc* 93:167–189, 1971
32. GHITESCU L, FIXMAN A, SIMIONESCU M, SIMIONESCU N: Specific binding sites for albumin restricted to plasmalemmal vesicles of continuous capillary endothelium: Receptor mediated transcytosis. *J Cell Biol* 102:1304–1311, 1986
33. GHINEA N, FIXMAN A, ALEXANDRU D, POPOV D, HASU M, GHITESCU L, ESKENASY M, SIMIONESCU M, SIMIONESCU N: Identification of albumin-binding proteins in capillary endothelial cells. *J Cell Biol* 107:231–239, 1988
34. SCHNITZER JE: gp60 is an albumin-binding glycoprotein expressed by continuous endothelium involved in albumin transcytosis. *Am J Physiol* 262:H246–H254, 1992
35. BUMBASIREVIC V, PAPPAS GD, BECKER RP: Endocytosis of serum albumin-gold conjugates by microvascular endothelial cells in rat adrenal gland; regional differences between cortex and medulla. *J Submicrosc Cytol Pathol* 22:135–145, 1990
36. SCHNITZER JE: Antibodies to SPARC inhibit albumin binding to SPARC, gp60 and microvascular endothelium. *Am J Physiol* 263: H1872–H1879, 1992
37. SCHNITZER JE, SUNG A, HORVAT R, BRAVO J: Preferential interaction of albumin binding proteins, gp30 and gp18, with conformationally modified albumin. Presence in many cells and tissues with a possible role in catabolism. *J Biol Chem* 267:24544–24553, 1992
38. SCHNITZER JE, BRAVO J: High affinity binding, endocytosis and degradation of conformationally modified albumins. Potential role of gp30 and gp18 as novel scavenger receptors. *J Biol Chem* 268:7562–7570, 1993
39. LEAK LV: Distribution of cell surface charges on mesothelium and lymphatic endothelium. *Microvasc Res* 31:18–30, 1986
40. GOTLOIB L, BAR-SELLA P, JAICHENKO J, SHOSTAK A: Ruthenium-red stained polyanionic fixed charges in peritoneal microvessels. *Nephron* 47:22–28, 1987
41. GOTLOIB L, SHOSTAK A, JAICHENKO J: Ruthenium-red stained anionic charges of rat and mice mesothelial cells and basal lamina. The peritoneum is a negatively charged dialyzing membrane. *Nephron* 48:65–70, 1988
42. TSILIBARRY EC, WISSIG SL: Absorption from the peritoneal cavity. SEM study on the mesothelium covering the peritoneal surface of the muscular portion of the diaphragm. *Am J Anat* 149:127–133, 1977
43. GHINEA N, ESKENASY M, SIMIONESCU M, SIMIONESCU N: Endothelial albumin binding proteins are membrane-associated components exposed on the cell surface. *J Biol Chem* 264:4755–4788, 1989
44. ESPERANCA MJ, COLLINS DL: Peritoneal dialysis efficiency in relation to body weight. *J Ped Surg* 1:162–169, 1966
45. CASLEY-SMITH JR: The dimensions and numbers of small vesicles in cells, endothelial and mesothelial, and the significance of these for endothelial permeability. *J Microsc* 90:251–269, 1969
46. GOTLOIB L, GARMIZO AL, VARKA I, MINES M: Reduction of vital capacity due to increased intra-abdominal pressure during peritoneal dialysis. *Perit Dial Bull* 1:63–64, 1981
47. CASLEY-SMITH JR: The influence of tissue hydrostatic pressure and protein concentration on fluid and protein uptake by diaphragmatic initial lymphatics: Effect of calcium dobesilate. *Microcir Endothel Lymphatics* 2:385–415, 1985
48. MAJNO G, PALADE GE: Studies on inflammation. I. The effect of histamine and serotonine on vascular permeability. An electron microscope study. *J Biophys Biochem Cytol* 11:571–606, 1961
49. SHEPRO D: Endothelial cells, inflammatory edema, and the microvascular barrier: Comments by a free radical. *Microvasc Res* 36:247–264, 1988
50. GOTLOIB L, SHOSTAK A, JAICHENKO J: Loss of mesothelial electronegative charges during murine septic peritonitis. *Nephron* 51:77–83, 1989
51. SHASBY MD, SHASBY SS: Active transendothelial transport of albumin: Interstitium to lumen. *Circ Res* 57:903–908, 1985
52. KREDIET RT, STRUIJK DG, KOOMEN GCM, HOEK FJ, ARISZ L: The disappearance of macromolecules from the peritoneal cavity during continuous ambulatory peritoneal dialysis (CAPD) is not dependent on molecular size. *PD Int* 10:147–152, 1990